Intercontinental Geoinformation Days

http://igd.mersin.edu.tr/2020/

Bathymetry analysis with use of Sentinel-2 images

Hakan Uzakara *1, **Nusret Demir** 1

1Akdeniz University, Faculty of Science, Department of Space Sciences and Technologies, Antalya, Turkey

Keywords
Remote sensing
Bathymetry
LIDAR
Sentinel-2

ABSTRACT

Bathymetry is described as Sea and Ocean depth measurements, and performed by many methods. Traditional methods, which are still used from the past to the present, have been replaced by modern methods with the development of technology. Sonar systems, LIDAR and remote sensing systems are listed as examples of these modern methods. The use of acoustic systems or LIDAR, are not economical in terms of both time and cost. In this study, remote sensing methods are investigated in order to minimize the time and cost. It is aimed to extract the information about bathymetry with use of free of charge satellite images. As input data, Sentinel-2 satellite images of the study area and reference bathymetry points from predefined locations, were used. Band ratio and multi-band methods are used, and the results were evaluated.

1. INTRODUCTION

Remote sensing is a science that provides information about the natural and artificial objects of the earth and evaluates them, without physical contact with the objects by using several platforms including satellites. It provides fast and economical solutions for many cases including land use, agriculture and marine studies etc..

In the literature, bathymetry are generally obtained from sonar devices, lidar data and satellite images. Although satellite-derived bathymetry does not have sonar or lidar accuracy, its large field capability, low cost and allowing analysis for areas where are not contacted easily (Gao 2009). To overcome the difficulties and disadvantages of these traditional methods, satellite-based remote sensing techniques have been developed (Pacheco et al. 2015) Basically, satellite-derived bathymetry is based on the relationship between reflected energy and water depth. For each pixel of the satellite image, there is a statistical relationship between the amount of energy detected by the sensor and the depth of the water at that pixel location. This relationship can be utilized with various calculation algorithms (Kumari and Ramesh 2020). Most of these algorithms require reference points which include about the depth (Jawak and Luis 2015).

Satellite images have different spatial resolution (+100 m - 31 cm). Only images with a resolution higher than 30 m are suitable since bathymetry derived from satellite images are based on average depth per pixel (Bailly du Bois 2011). High resolution (less than a few meters) satellites such as WorldVIEW-2 and RapidEye for deriving bathymetry from satellite images, medium resolution (10 - 30 m) satellites such as Landsat-8 and Sentinel-2, 3 are increasingly being tested for bathymetry analysis of shallow regions (Caballero and Stumpf 2019) (Stumpf et al. 2003). The spatial and spectral resolution of satellite images used in bathymetry analyzes, satellite viewing angle, atmospheric effects, tidal level, sunlight and vegetation affect the accuracy. Some of these effects can be overcome by preciese selection of satellite images and image processing (Kumari and Ramesh 2020). In this study, bathymetry analysis was performed with free use of Sentinel-2 images, which are freely available thorugh ESA Copernicus program.

2. METHOD

2.1. Study Area

The study area has been selected from the coastal zone of the city of Los Angeles in the state of California, USA. The coordinates of the study area are located at latitudes North = 33.747, West = 118.412, South = 33.62, East = 118.285.

* Corresponding Author

*(hakanuzakara@gmail.com) ORCID ID 0000 – 0001 – 9985 – 832X
(nusretdemir@akdeniz.edu.tr) ORCID ID 0000 – 0002 – 8756 – 7127

Cite this study

Uzakara H & Demir N (2020). Bathymetry analysis with use of Sentinel-2 images. Intercontinental Geoinformation Days (IGD), 21-24, Mersin, Turkey

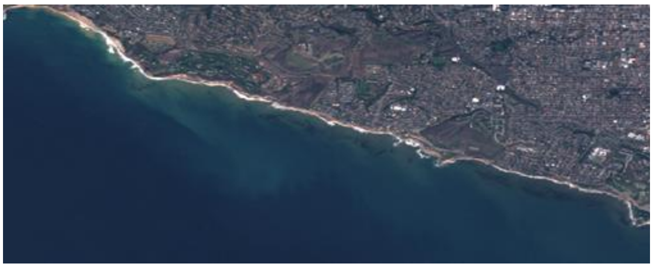

Figure 1. Study area

As a result of preliminary analysis in the region, it has been determined that there is a large amount of chlorophyll and similar structures in areas up to 10 meters from the shore. Since these cause deviations in spectral reflections, regions with a depth of 10 meters to 30 meters were chosen as the study area.

2.2. Materials

Sentinel-2 satellite images of the study area were downloaded from ESA's Copernicus platform. Sentinel-2 MSI is a polar-orbit, multispectral high-resolution satellite that aims to perform field analyzes such as vegetation, soil and water cover areas. Sentinel-2A started operations on June 23, 2015, and Sentinel 2B on March 7, 2017.

Table 1. Sentinel-2 satellite band features

Band	Name	Central wavelength (nm)	Spatial resolution (m)
1	Aerossol	443	60
2	Blue	490	10
3	Green	560	10
4	Red	665	10
5	Red Edge 1	705	20
6	Red Edge 2	740	20
7	Red Edge 3	783	20
8	NIR	842	10
9	Cirrus	945	60
10	SWIR 1	1380	60
11	SWIR2	1610	20
12	Red Edge 4	2190	20

Reference bathymetry data of the analysis area was obtained from TCarta Global Bathymetry GIS Data site at 10m resolution.

2.3 Method

The analysis is directly dependent on solar radiation. Absorption, scattering and reflection occur when solar radiation reaches the water surface. The energy of the light entering the water body will be reflected from the base and reach the sensor. Depth estimation can be made as a function of light reflected from underwater using bands of different wavelengths. Depth was estimated using different band combinations in the study. Different combinations were obtained by using blue, green and red spectral bands. The interaction of each band with the water column has different reflection properties, which is an important factor in improving accuracy in depth estimation.

2.3.1 Dual band ratio method

The bottom reflectance of the two bands does not change with the type of substrate. This can eliminate the influence of water type and the ratio of the two bands can be used to calculate water depth (Chen et al. 2019; Bramante et al. 2012).

$$Z = m_0 * \frac{ln\, ln\left(R_w(\lambda i)\right)}{ln(R_w(\lambda j))} - m_1 \quad (1)$$

Equation (1) λi and λj are the reflection values of the bands. For the equation to be positive in all conditions, n is a constant number. The reference bathymetric depths will be written instead of z and the m1 and m0 coefficients will be found. By using the coefficients found, a depth estimation is aimed for areas of unknown depth. This method is based on the absorption of each tape into a different body of water. These different absorptions create a ratio between the bands. These rates theoretically increase as the depth increases.

2.3.2 Multi band method

The multi-band model represents more than one aspect of water depth (Stumpf et al. 2003). Z reference depth values, spectral reflection values of the R_n n band, a are indeterminate coefficients.

$$Z = a_0 + a_1 ln(R_1) + a_2 ln(R_2) + \ldots + a_n ln(R_n) \quad (2)$$

The above equation calculates unknown coefficients a_n by multiple regression analysis, using R_n bands against reference depth values.

2.3.3 Accuracy Evaluation

The results obtained from both models were evaluated with absolute error (D_a), relative error (D_b) and RMSE (D_c).

$$D_a = \frac{|z_1 - z_2|}{n} \quad (3)$$

$$D_b = \frac{\sum_1^n \left|\frac{z_1 - z_2}{z_1}\right|}{n} \quad (4)$$

$$D_c = \sqrt{\frac{\sum_1^n (z_1 - z_2)^2}{n}} \quad (5)$$

z_1 represents the actual depth value, z_2 represents the calculated depth value n and the sample size.

3. RESULTS

Correlation analysis was performed between reference bathymetry values and band combinations to determine the most appropriate method and band combination. Table 2 below shows the calculated correlation coefficients.

In the multi-band model, the best correlation was obtained with the combination of blue, green and red bands. In the double band ratio model, the lowest is obtained from the ratio of blue band to green band. In general, it is seen that the correlation coefficients are significant. Equation 1. regression analysis and Equation 2. As a result of multiple regression analysis, the depth estimation of the analysis area was made by calculating the m and a coefficients.

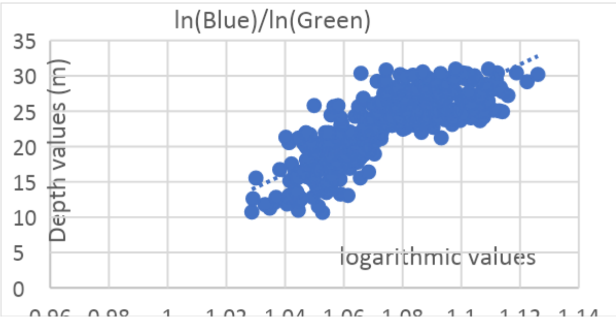

Figure 2. Band rate distribution

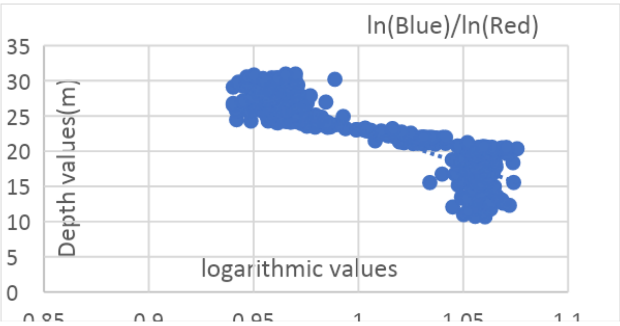

Figure 4. Band rate distribution

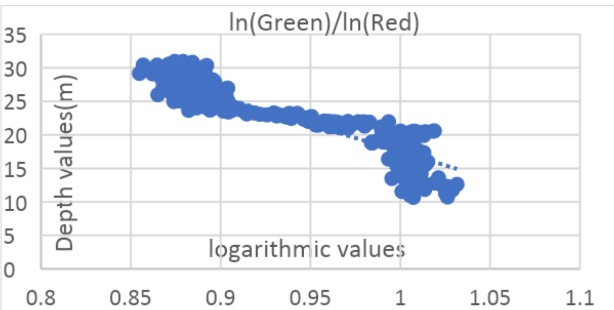

Figure 5. Band rate distribution

As shown in Figures 3, 4, 5, the (blue) / ln (green) band ratio values fit better along the regression line compared to the other graphs. In ln (blue) / ln (red) and ln (green) / ln (red) band combinations, scattering from the regression line is observed in regions with a depth of 10 to 15 meters and 25 to 30 meters. . The factors causing these scattering are the fact that the red spectral band has more absorption in the water column than the other bands, resulting in a narrower spectral reflection values. This narrow spectral reflection range is thought to cause scattering in the regression line in combinations with the red band.

Using the coefficients calculated by regression analysis, Equation 1 and Equation 2 depth estimation was made at points of unknown depth.

Figure 3. Reference bathymetry map of the study area

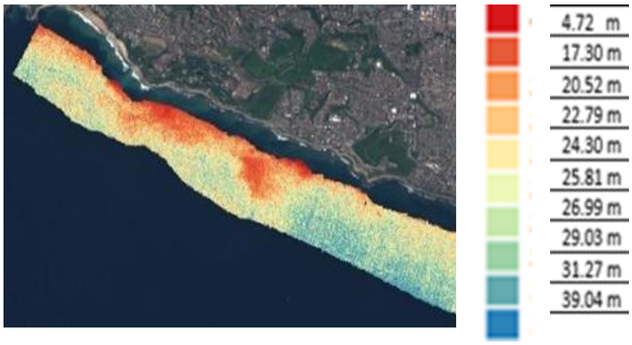

Figure 4. ln (blue) / ln (green) forecast bathymetry map

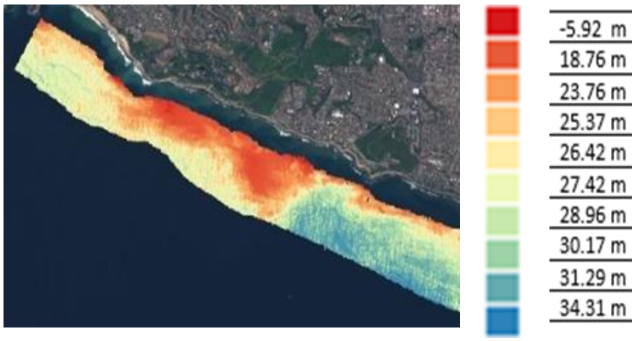

Figure 5. ln (green) + ln (blue) + ln (red) forecast bathymetry map

It has been observed that the estimated bathymetry maps generally have values close to each other. The best correlation was obtained from multiple regression analysis with a combination of blue, green, and red bands. The lowest correlation was calculated from the ratio of the blue band to the green band. The error from the blue, green and red band combination with the best correlation is higher than the error from the ratio of the blue band to the green band with the lowest correlation (Table 2). The reason for this error is the changes in the spectral reflection of the red band associated with the water column.

Table 2. Correlation and error of band groups

Models	Dual band ratio method			Multi band method	
	ln(blue)/ ln(green)	ln(blue) / ln(red)	ln(green)/ ln(red)	ln(blue) / ln(green)	ln(blue)+ ln(green)+ ln(red)
Correlation	0.802	-0.884	-0.913	0.966	0.968
Absolute error	5.364	5.429	5.431	5.607	5.951
Relative error(%)	30.199	32.883	32.233	32.913	34.669
RMSE	6.565	6.835	6.722	6.909	7.305

4. DISCUSSION

This study demonstrates the potential of Sentinel-2 satellite images to predict bathymetry at 10 m spatial resolution for Los Angeles coastal regions in low turbidity conditions. Batimetry products derived from satellites can be obtained in both models. Several researchers report that the methods are successful in shallow water areas of approximately 15 m (Kerr and Purkis 2018)

Bathymetry data derived from satellites can be used as reference data in remote areas, hard-to-reach areas or areas not drilled. Therefore, bathymetry can be considered as a potential technology in areas where research is not conducted or is insufficient.

The red band at 665nm (B04) has a narrow reflection range as a result of its interaction in the water column. This caused more scattering than other band combinations (Figure 4.) in regions with depths of 10 m and 15m and 25 m and 30m, resulting in outliers.

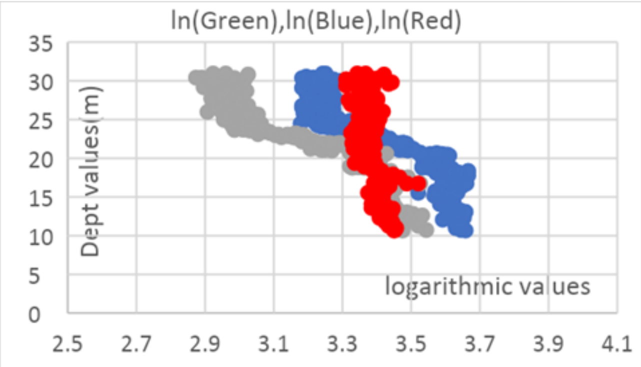

Figure 9. Logarithmic reflections of blue, green, red bands

5. CONCLUSION

In this study, Sentinel-2 demonstrates the ability to produce bathymetric maps with 10 m resolution with satellite images. The methods showed satisfactory results in shallow and less turbid waters. In band combinations with red band, it has been observed that the interaction of the red band with the water column causes more errors than the other combinations.

ACKNOWLEDGEMENT

This work has been supported by General Directorate of Mapping Turkey. Authors acknowledge the datasets provided by Sentinel Copernicus and TCARTA.

REFERENCES

Bailly du Bois P (2011). Automatic calculation of bathymetry for coastal hydrodynamic models. Computers & Geosciences, *37*(9), 1303-1310. https://doi.org/10.1016/j.cageo.2010.11.018

Bramante J F, Raju D K & Sin T M (2012). Multispectral derivation of bathymetry in Singapore's shallow, turbid waters. International Journal of Remote Sensing, *34*, 2070-2088. https://doi.org/10.1080/01431161.2012.734934

Caballero I & Stumpf P R (2019). Retrieval of nearshore bathymetry from Sentinel-2A and 2B satellites in South Florida coastal waters. Estuarine, Coastal and Shelf Science, *226*, 106-277. https://doi.org/10.1016/j.ecss.2019.106277

Chen B, Yang Y X D & Huang E (2019). A dual band algorithm for shallow water depth retrieval from high spatial resolution imagery with no ground truth. ISPRS Journal of Photogrammetry and Remote Sensing, *151*, 1-13. https://doi.org/10.1016/j.isprsjprs.2019.02.012

Gao J (2009). Bathymetric mapping by means of remote sensing: Methods, accuracy and limitations. Progsress in Physical Geography, *33*(1), 103-116.

Jawak S D & Luis A J (2015). Spectral Information Analysis for the Semiautomatic Derivation of Shallow Lake Bathymetry Using High-resolution Multispectral Imagery: A Case Study of Antarctic Coastal Oasis and Aquatic Procedia, *4*, 1331-1338. https://doi.org/10.1016/j.aqpro.2015.02.173

Kerr J M & Purkis S (2018). An algorithm for optically-deriving water depth from multispectral imagery in coral reef landscapes in the absence of ground-truth data. Remote Sensing of Environment, *210*, 307-324. https://doi.org/10.1016/j.rse.2018.03.024

Kumari P & Ramesh H (2020). Remote sensing image based nearshore bathymetry extraction of Mangaluru coast for planning coastal reservoir. Sustainable Water Resource Development Using Coastal Reservoirs, 247-265. https://doi.org/10.1016/B978-0-12-818002-0.00013-7

Pacheco A, Horta J, Loureiro C & Ferreira Ó (2015). Retrieval of nearshore bathymetry from Landsat 8 images: A tool for coastal monitoring in shallow waters. Remote Sensing of Environment, 102-116. https://doi.org/10.1016/j.rse.2014.12.004

Stumpf P R, Holderied K & Sinclair M (2003). Determination of water depth with high-resolution satellite imagery over variablebottom types. Limnol and Oceanog, *48*(1), 547-556. https://doi.org/10.4319/lo.2003.48.1_part_2.0547